DIMENSIONAL STABILITY OF SUBSTRATES FOR PRINTED ELECTRONICS

By

Dilwyn P. Jones
Emral Ltd.
UNITED KINGDOM

ABSTRACT

Substrates for flexible displays must retain registration between multiple process steps. Although polyester substrates offer cost and handling advantages, their dimensions are affected by tension, temperature and humidity. This paper will summarize the understanding of viscoelasticity, thermal and hygroscopic expansion, shrinkage, and their anisotropy in polyester. Thermomechanical and Dynamic Mechanical Analysis data are particularly useful to understand and predict substrate behavior.

These effects have been mitigated in sheet processing by laminating the film to a glass sheet: however, a thermal cycle produces bowing distortion that can make subsequent steps impossible. A model for the development of bow from differential thermal expansion, and its relaxation and setting-in by the viscoelastic polymer layer properties, will be outlined. The bow direction and trends are predicted well but the absolute accuracy is not perfect. The model is useful in developing thermal and constraint conditions during fabrication.

Finally, key points for maintaining dimensional stability and preventing wrinkles during roll to roll processing will be summarized. It is particularly important to control tension during drying steps at elevated temperature: high levels can obliterate the benefits of expensive “heat-stabilized” substrates.

NOMENCLATURE

DMA	Dynamic Mechanical Analysis
MD	Machine Direction, i.e. along direction of travel
PEN	Poly(ethylene naphthalate)
PET	Poly(ethylene terephthalate)
ppm	Parts per million
RH	Relative Humidity
TD	Transverse Direction, i.e. across the web
TMA	Thermomechanical Analysis

TTS	Time-Temperature Superposition
VBA	Visual Basic® for Applications
WLF	Williams-Landel-Ferry model for TTS
a(T)	Time-temperature shift factor
C_{11}, C_{12} etc.	*xx* and *xy* components of the stiffness tensor
C_0	Time-independent term of a stiffness tensor component
C_k	k^{th} time-dependent stiffness tensor component term
e	The base of natural logarithms, 2.718
$E(t)$	Time-dependent stress relaxation modulus
$E_1(t)$	Time-dependent MD stress relaxation modulus
$E_2(t)$	Time-dependent TD stress relaxation modulus
E_0	Time-independent term of stress relaxation modulus
E_k	k^{th} time-dependent stress relaxation modulus term
I	Integral in equation 6 or 7
j	Timestep index
k	Relaxation term index
k_x, k_y	MD and TD curvature of stack
l	Panel length
N_k	Number of relaxation terms
r	Heating rate in the TMA
R	Stack curl radius
s	Slope of the TTS log(shift factor) versus temperature curve
S_k	k^{th} time-dependent shrinkage strain term
t	Time
t_r	Reduced time
t', t_r'	Dummy variables for time, reduced time
t_j	Time at the timestep *j*
T	Temperature
T_r	Reference temperature for TTS
x, y	Coordinates in MD and TD
z	Through-thickness coordinate, with origin at the lower stack surface
Z	Total stack thickness
$\alpha_x(T)$	MD coefficient of linear thermal expansion at temperature *T*
β_{kj}	k^{th} memory term in a stress integral at timestep *j*
ε	Strain
ε_x, ε_y	*x*- and *y*- components of strain
$\varepsilon_x{}^m$	*x*-component of mechanical strain
$\varepsilon_x{}^t$	*x*-component of thermal strain
$\varepsilon_x{}^s$	*x*-component of shrinkage strain (positive is expansion)
$\varepsilon_x{}^i$	Initial strain in *x* direction
$\varepsilon_x{}^0$	*x*-component of strain, equal in all layers, required to give zero net force or bending moment
ν	Poisson's ratio; in anisotropic material, the contraction in *y* when *x*-stress is applied.
σ	Stress
σ_x, σ_y	*x*- and *y*- components of stress
τ_k	k^{th} relaxation time in the fit of stress relaxation master curve

Δt_j	Time interval in step j
$\Delta \varepsilon^m{}_j$	Change in mechanical strain during step j

INTRODUCTION

Polymer substrates for plastic electronics generally have poorer dimensional stability when heated and cooled than traditional semiconductors such as silicon [1]. This may cause problems when registration of several precise process steps is needed. The dimensions of features may change after they are laid down. The changes are caused by mechanical stress, temperature and changes in ambient moisture, often during a drying or curing step.

Flexible substrates are used because a roll to roll process offers economic advantages [2], or because flexibility is a key attribute of the final product, for example rollable displays [3]. In the second case, sheet processes can be used with the substrate mounted on a more rigid sheet such as silicon or glass. However, this method is still affected by the dimensional stability of the substrate, as will be demonstrated later in this paper.

Bending flexibility and zero in-plane dimension change under stress are mutually exclusive! Instead, the ideal substrate will have a purely elastic response to stress, coupled with reversible thermal and moisture expansion. Then, it will return to its original dimensions provided that the stress, temperature and humidity reproduce their original values closely enough, and enough time is allowed for equilibration. However, polymer substrates generally change dimension under these circumstances. Equipment can be compensated for a constant shift in dimensions, or an automatic system can position the second set of features by detecting the position of the first. Variations over the area of a single device are more difficult to deal with.

Despite these limitations, biaxially-oriented polyester films based on poly(ethylene terephthalate) (PET) and poly(ethylene naphthalate) (PEN) have been successfully used for many flexible electronic devices, including displays, lighting and solar cells [4]. Reference [5] contains a comprehensive review of properties important for an earlier demanding application, magnetic media. The oriented, semi-crystalline morphology confers reasonably high modulus, low creep at room temperature, and a reasonable temperature range for processing. However, once temperature rises above the glass transition (78 and 120 deg C for PET and PEN respectively), stresses must be kept low to avoid significant creep, after which the strain is “frozen in” and the specimen length increases. Also, when hot, the film as-made shrinks irreversibly in both directions. Additional heat-stabilization is carried out to reduce the shrinkage [6].

The first part of this paper focusses on the fundamental properties that underlie dimensional stability issues. Film manufacturers rarely give more information than Young’s modulus and coefficient of thermal expansion in machine and transverse directions (MD and TD), and the amount of shrinkage after exposing the film to a particular temperature (e.g. 150 deg C for 30 minutes). The measurement and interpretation of more fundamental properties can become very involved: the approach here provides a framework that can be used for both quantitative calculations and qualitative understanding of processes.

The second part describes the application of the measured properties to a process for flexible display production. The polyester substrate is attached to a glass sheet to make a panel that is processed using standard semiconductor tools, some of which involve a “bake” at elevated temperature. However, the panel may distort into a “bow” shape as a result of a bake, which may disrupt further processing, if the panel cannot be held on a vacuum table, for example. A computer model of the process was written to predict the

amount of bow for different multilayer stacks subjected to the sequence of heating and cooling steps making up the bake under restraint or free.

The final part describes the behavior of film in a long unsupported span in an oven where the web is both heated and cooled. Conditions which lead to unwanted dimension change, trough and wrinkle formation are identified so they can be avoided.

WEB PROPERTIES

The properties of polymers depend not only on the name of the material, but also on the details of composition and manufacturing process. Users need to be aware that changing the supplier, grade and thickness can affect the performance of the substrate. Typical specifications are broad, and may not have been established for specialized applications such as flexible electronics. Mapping out all aspects of dimensional stability would be a very time-consuming and costly exercise. Instead, a streamlined approach, proposed here, leads to a set of properties that can be used for quantitative predictions, including mathematical models, and a more pictorial understanding of web behavior.

Viscoelastic Behavior

Polymer films have a time-dependent response to stress, even for the lowest values [7]. Three manifestations are shown in Figure 1. Application of load (stress) leads to a gradually increasing strain (creep). When the load is removed, the strain gradually recovers. Secondly, rapid application of strain generates a stress that falls (relaxes) with time. Returning to zero strain reverses the direction of stress, which then decays towards zero. Thirdly, in an oscillatory test, strain lags behind stress. The in-phase component represents storage of recoverable energy, and the out-of phase component energy loss or dissipation. This combination of elastic and viscous behavior is described by a viscoelastic response.

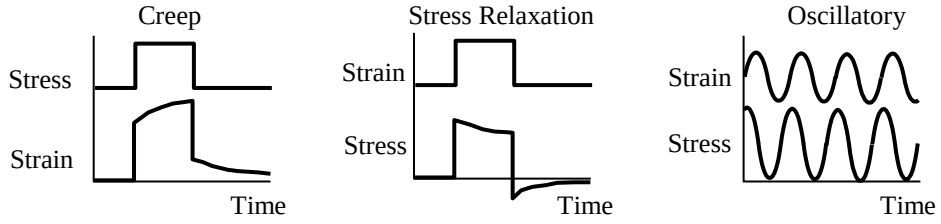

Figure 1 – 3 manifestations of viscoelastic behavior.

Standard tests for Young's modulus of polymers usually employ a linear increase of strain with time [8]. Viscoelastic behavior leads to curvature of the stress-strain plot even close to the origin, and a dependence on fitted slope with strain rate. The modulus value falls with increasing temperature: this too is a consequence of viscoelastic behavior.

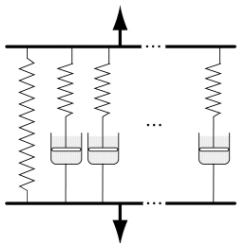

Figure 2 – Spring and dashpot model for viscoelastic solid.

At small strains, creep, stress relaxation and oscillatory tests show a linear relationship between stress and strain, and a superposition principle can be applied for loading sequences. The behavior is described by a model consisting of an arrangement of springs and dashpots. For stress relaxation, the easiest representation is to have a number N_k of Maxwell elements in parallel (figure 2). Strain is applied to all elements equally. The stress σ falls quickly in those with low dashpot viscosity, and slowly with high viscosity. Each element stress decays exponentially with a relaxation time τ_k and contributes an amount E_k to the initial stress, so the response to a strain ε imposed at t=0 is given by:

$$\sigma = E(t)\varepsilon = \left(E_0 + \sum_1^{N_k} E_k e^{-t/\tau_k}\right)\varepsilon \qquad \{1\}$$

Polymers are characterized by a very broad spread of relaxation times, covering many orders of magnitude. This reflects the range of sizes and local environments of chain segments in the disordered amorphous phase of the material. In practical tests, there are always some elements that respond elastically and others whose stress decays very quickly. The "instantaneous" or elastic response in a test is not a true property, and depends on how quickly the load is applied. Any fit to data produces a constant E_0 that includes all elements that do not relax in the experimental timescale.

The results of different tests are related in simple viscoelastic materials, and the most appropriate representation can be chosen for measurement and modelling. Full and accurate characterization of stress relaxation and creep requires specialized equipment and lengthy experimental programs, as reviewed in [5]. However, thermal analysis instruments can be used to generate data quickly by testing for short durations at a range of temperatures.

Time-Temperature Superposition

The tests reported here were carried out using Dynamic Mechanical Analysis (DMA) in stress relaxation mode [9]. A 5 mm wide specimen was clamped at both ends, leaving a 15 mm gauge length. It was mounted in the instrument, surrounded by a furnace. A thermocouple next to the specimen monitors temperature and feeds back to the furnace to control temperature as required. A flow of dry air or nitrogen is used to promote thermal equilibration and prevent moisture absorption. A small preload of 1 mN was applied to keep the specimen taut prior to the application of the test strain. The temperature was ramped up to the each new test temperature then held at the value for 10 minutes. The test strain of 0.2% was applied for 30 minutes, recording the load as a function of time. A complete set of data from 10 to 150 deg C took a day to acquire.

Typical results are shown in figure 3, with the load converted to modulus. Stress decays with time at each temperature. Behavior close to room temperature is nearly

elastic, but there is still some stress relaxation. The strongest time dependence occurs between 60 and 110 deg. C. At higher temperatures, the modulus is small but only decays weakly during the test.

Time-temperature superposition (TTS) allows the viscoelastic performance to be predicted outside the range of experimentally measured times [7]. The procedure was carried out manually using Microsoft Excel®. The curves in figure 3 were replotted on a logarithmic time scale, then a horizontal shift applied to each curve in turn to coincide with the "master curve" as it builds up. A reference temperature of 50 deg C was chosen: this curve is not shifted. The resulting superposed curves are shown in figure 4, extending over 18 orders of magnitude in time.

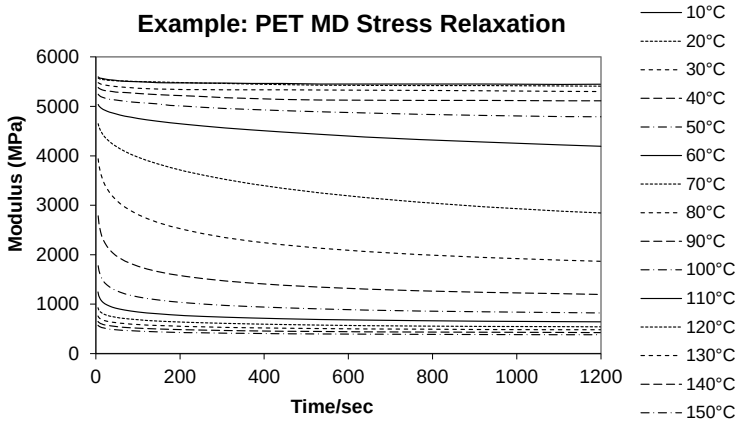

Figure 3 – Typical stress relaxation curves for PET film at different temperatures.

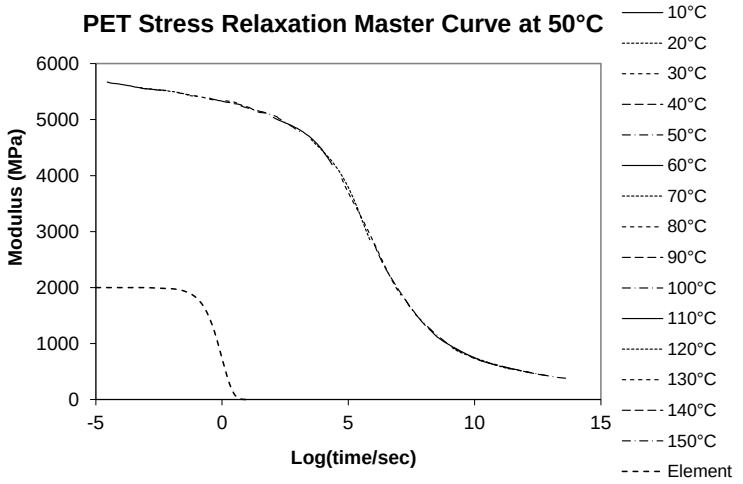

Figure 4 – PET stress relaxation curves at different temperatures superposed by a horizontal shift to produce a master curve. The dashed line shows the response of a single Maxwell-Kelvin element.

This "master curve" is fitted (using Excel® Solver) to the sum of terms in equation 1, finding the E_k values for relaxation times of 0.001, 0.01,…10^{17} sec. Figure 4 also shows the response of an element with relaxation time 1 sec, showing it is very much narrower than the broad response of the material. Modern DMA instruments offer automated TTS analysis.

The shift factor relates the "reduced time" t_r at the reference temperature T_r to time *t* at an actual temperature *T*.

$$t_r = a(T)t \quad \{2\}$$

A plot of log(shift factor) versus temperature is shown in figure 5. The dependence is linear below 110 deg C, and is represented by:

$$\log_{10}(a(T)) = s(T - T_r) \quad \{3\}$$

The slope *s* is 0.128 K^{-1}, so a 10-fold increase in time is equivalent to a temperature drop of 8 deg C.

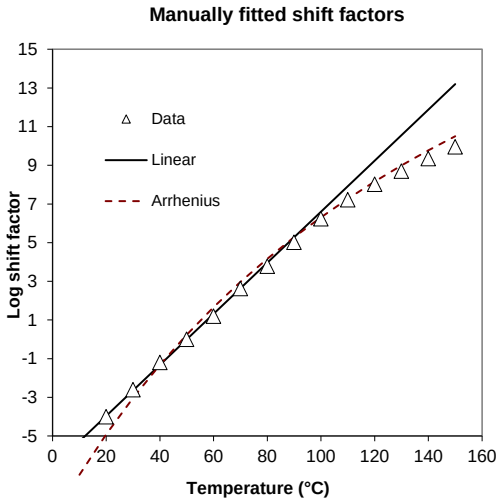

Figure 5 – Shift factors as a function of temperature for the curves in figure 4, showing data and fits to a straight line and Arrhenius dependence.

2-Dimensional Viscoelastic Parameters

To understand the interaction of forces, constraints and bending in both MD and TD, a set of constitutive equations is needed. Experimental MD and TD stress relaxation curves differ somewhat, much like the quoted Young's moduli, implying some anisotropy. For an elastic material, the equations are:

$$\sigma_x = C_{11}{\varepsilon_x}^m + C_{12}{\varepsilon_y}^m \quad \{4\}$$

$$\sigma_y = C_{12}{\varepsilon_x}^m + C_{22}{\varepsilon_y}^m \quad \{5\}$$

The corresponding set for viscoelasticity is:

$$\sigma_x = \int^{t_r} C_{11}(t_r - t_r') \frac{d\varepsilon_x{}^m}{dt_r'} dt_r' + \int^{t_r} C_{12}(t_r - t_r') \frac{d\varepsilon_y{}^m}{dt_r'} dt_r' \quad \{6\}$$

$$\sigma_y = \int^{t_r} C_{12}(t_r - t_r') \frac{d\varepsilon_x{}^m}{dt_r'} dt_r' + \int^{t_r} C_{22}(t_r - t_r') \frac{d\varepsilon_y{}^m}{dt_r'} dt_r' \quad \{7\}$$

The terms add together the contributions from the strain history up to the current time *t* by integrating over the dummy reduced time variable t_r'.

The stiffness terms C_{11}, C_{22} should relate to tests with no change in width. However, the experimental measurements E_1, E_2 allow width contraction according to Poisson's ratio. There are very few measurements of Poisson's ratio [10], but a value of 0.3 is frequently assumed. Assuming this applies for the TD width contraction when load is applied in the MD at all times, allows all the stiffness terms to be estimated:

$$C_{11}(t) = \frac{E_1(t)}{1-\nu^2 E_2(0)/E_1(0)} \quad \{8\}$$

$$C_{22}(t) = \frac{E_2(t)}{1-\nu^2 E_2(0)/E_1(0)} \quad \{9\}$$

$$C_{12}(t) = \nu C_{22}(t) \quad \{10\}$$

This lengthy procedure finally gives functions that can be used for modelling.

More sophisticated approaches

The above approach was driven by the need to develop a model for bowing quickly in an industrial development environment. More sophisticated approaches could be taken, for example:

- Fit the TTS shift factors to a different temperature dependence, such as Arrhenius or Williams-Landel-Ferry (WLF) [11].
- Use vertical as well as horizontal shifts in TTS. This leads to some of the constants E_k in equation 1 depending on temperature.
- Use 2 or more sets of relaxation times, shifting in different ways with temperature. Examples could include shear and volumetric deformation of the amorphous phase, and crystal slip.
- Bring in non-linearity to allow a decrease in relaxation times under tension caused by opening up the structure, and an increase under compression [12].
- Add in non-recoverable (plastic) deformation. Most studies of recovery stop too early to assess whether this occurs or not.

The constitutive equations have not been checked here by carrying out other experiments. It is important for the models that the equations fit not only stress relaxation, but also recovery after load is removed, and that the long-term behavior is predicted reasonably well from the master curve. Ensuring that the creep, stress relaxation and oscillatory tests lead to the same constitutive equation parameters would also give confidence to the approach.

Dimension Changes from Temperature

Manufactures normally quote MD and TD values of the coefficient of linear thermal expansion at room temperature, and of shrinkage developed after holding a specimen unrestrained for 5 minutes at an elevated temperature, often 120 or 150 deg C.

The behavior of film as temperature changes can be understood by using Thermomechanical Analysis (TMA). The specimen environment is similar to the DMA, and its length is measured as temperature is programmed through a succession of ramps and hold times [13]. Figure 6 shows the TMA used to replicate a 180 deg C shrinkage test on normal PET, with a heating rate of 5 deg/min.

The film expands up to 80 deg C, but then shrinks on further heating. It is around 1% shorter at 180 deg C than its original length. On cooling, there is further contraction, giving a net length reduction of 1.9% on return to room temperature.

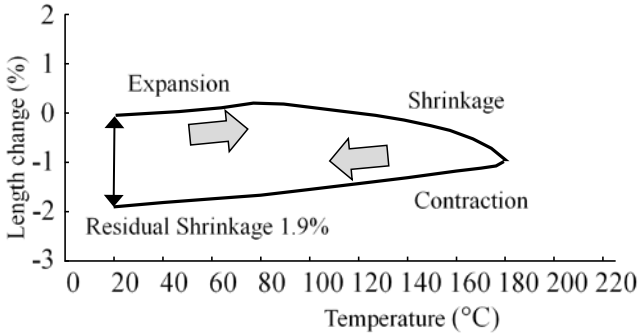

Figure 6 – Length changes in PET film during cycling to 180 deg C, measured by TMA.

For applications where dimensional stability is required, manufacturers supply "heat-stabilized" film with reduced shrinkage in the TD alone or both directions. Figure 7 shows the TMA trace of stabilized film under the same conditions with an expanded vertical scale, displaying expansion on heating and contraction on cooling. Shrinkage on heating does not occur. The net dimension change is an increase of 0.1%.

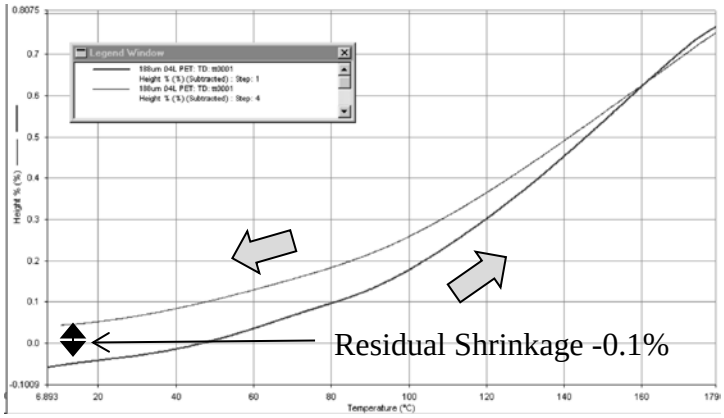

Figure 7 – TMA instrument trace of length changes in stabilized PET film during cycling to 180 deg C.

Further insight can be gained from a repeated cycling experiment, shown in figure 8. In the initial ramp up to 140 deg C, shrinkage develops above 80 deg C as before, and the specimen contracts on cooling. During the next ramp to 160 deg C, the length retraces the previous cooling curve up to 140 deg C, apart from a small shift attributed to thermal

lag. Shrinkage only develops once the previous maximum temperature is exceeded. Similar behavior occurs on subsequent cooling and heating to 180 and 200 deg C. A single heating ramp follows the outer envelope of the steps.

Shrinkage appears only on the first pass through a given temperature. Once it has developed, heating and cooling below that temperature follow the same curve. The cooling and reheating curves from different temperature are all parallel, attributed to an underlying, reversible, thermal expansion.

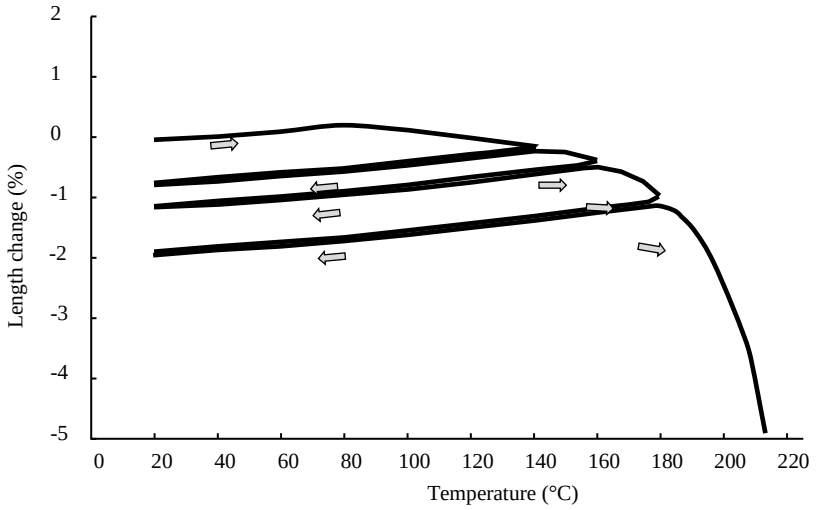

Figure 8 – Length changes in PET film during repeated cycling to increasing maximum temperature, measured by TMA.

Heating under low tension allows shrinkage to develop, and is said to relax or heat-stabilize the film because that shrinkage does not appear on subsequent reheating. It does not affect the reversible thermal expansion contribution, nor shrinkage developed above the stabilization temperature.

Viscoelastic Description of Shrinkage

As-manufactured polyester films shrink when they are heated above their glass transition temperature. If a specimen is held at fixed temperature in the TMA, shrinkage develops during the heating and also slowly during the hold time. Experiments on film that has been extended at high temperature show similar shrinkage behavior to as-made film [14]. This evidence suggests that shrinkage is a viscoelastic recovery phenomenon, with the initial strain provided during manufacture or deformation.

The biaxial orientation process heat-sets the film in ovens above 210 deg C. whilst held in clips, preventing contraction. This causes structural and conformation change in the polymer, with crystals growing and the amorphous orientation relaxing. Rather than returning to the unstretched dimensions of 25-30% of the stretched film, the film only seeks to contract by around 4% after heat-setting. Cooling under restraint freezes in most of this strain, and the contraction on release is only around 0.2%. The remaining 3.8% can be gradually recovered as shrinkage on heating.

The reversible thermal expansion and shrinkage curve can be measured on the TMA with an initial ramp, cooling, and then a reheat. The reheat gives the thermal expansion

contribution, with the coefficient normally increasing with temperature (figure 9). Subtracting this from the initial heating trace gives the shrinkage as a function of temperature (figure 10). To convert this to reduced time (figure 11), the incremental version of equation 2 is integrated to give:

$$t_r = \frac{10^{s(T-T_r)}}{rs\ln 10} \qquad \{11\}$$

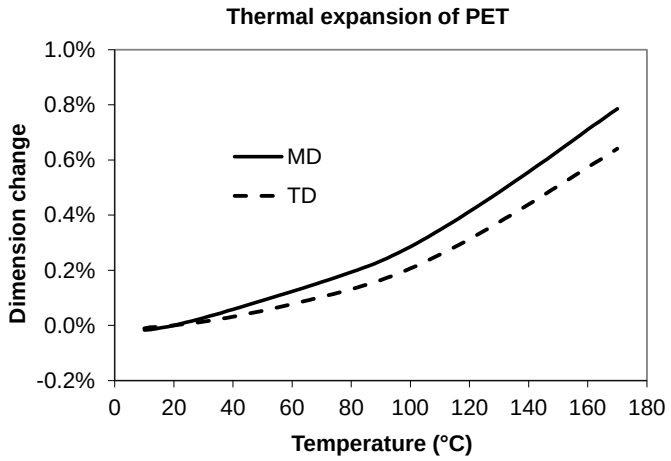

Figure 9 – Length changes in PET film due to thermal expansion, measured during a reheat temperature ramp using TMA.

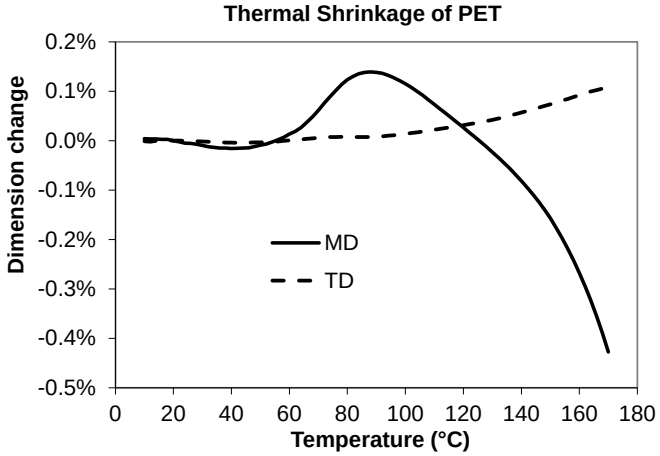

Figure 10 – Thermal shrinkage as a function of temperature, obtained by subtraction of reheat from initial heating trace on the TMA.

The example shows an expansion in the TD, and shrinkage at high temperature in the MD. There is quite a marked expansion in the MD around 100 deg C. The origin of this is not clear, as it would require MD compression to generate.

Moisture Effects

Polymers with polar groups such as polyesters and especially polyamides absorb moisture from their environment. Although water permeability is commonly measured, it is also important to know the solubility and diffusion coefficient. PET absorbs water in proportion to the relative humidity of the surroundings: 0.4 % by weight is absorbed at 80 % RH [15]. The solubility is independent of temperature up to 150 deg C. The rate at which equilibrium is attained depends on the film thickness and diffusion coefficient, itself dependent on temperature. Data on PEN are similar to PET [4].

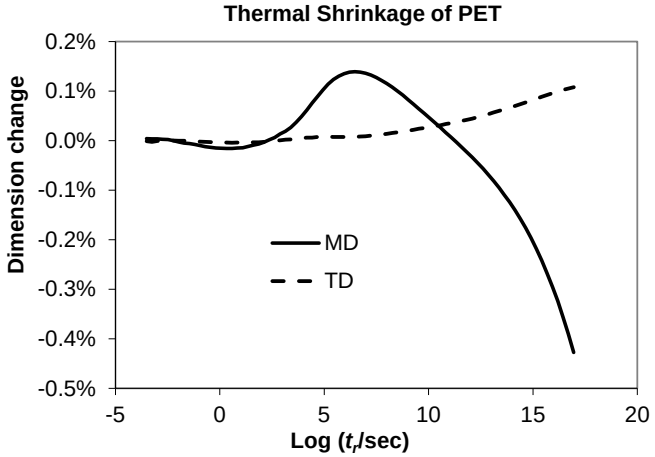

Figure 11 – Thermal shrinkage of PET, as shown in figure 10, replotted against reduced time calculated using the time-temperature shift factor.

Moisture absorption causes expansion in all directions, greater in directions of lower molecular orientation. The in-plane coefficient of hygroscopic expansion is around 7 ppm for a 1% RH change [16].

The absorbed moisture affects the mobility of polymer segments, and acts as a plasticizer to reduce viscoelastic relaxation times during creep. The limited data available [17] have been interpreted by applying a moisture shift factor, analogous to TTS. There is a factor of 10 reduction in relaxation time for a 20 to 40% increase in RH. The moisture shift factor varies with temperature, according to the data.

These effects are less important than temperature changes, but nevertheless should be considered for flexible electronics processing. Passing a polyester web through an oven will remove moisture because the RH will be low. This will cause contraction, which will reverse as the web slowly reabsorbs moisture at room temperature. There will be a difference between web from the inside and outside of a wound roll, because of the time it takes moisture to diffuse away from the surface.

Anisotropy and Orientation

Polyester films are described as “balanced” but are produced by a sequential draw process, where the orientation produced by the second (TD) draw is greater than the first (MD). A stable process with equal orientation proved impossible to achieve in early development. The principal directions of orientation are rotated from the MD and TD towards the web edges by the restraint conditions [6]. Figure 12 shows how lines drawn

across the film after the first draw form curves after the second, because the edges are held in clips while the center retracts under MD stress developed in the draw. The film elements towards the edge are subject to a combination of TD stretching and shear.

The principal directions of properties such as refractive index, modulus, thermal and moisture expansion vary from the MD and TD at the web center, to an orientation angle of around 40 degrees at the edges [16]. The orientation angle can be found easily by rotating the film between two polarizing sheets at right angles and finding the angle where no light is transmitted (extinction angle). The properties arise from the orientation distribution of crystals, whose c-axis has a higher stiffness than the others and negative coefficient of thermal expansion. One crystal population is close the machine direction, and a second forms at an angle. It is possible to relate properties to the crystal orientation distribution derived from wide-angle X-ray diffraction measurements [18].

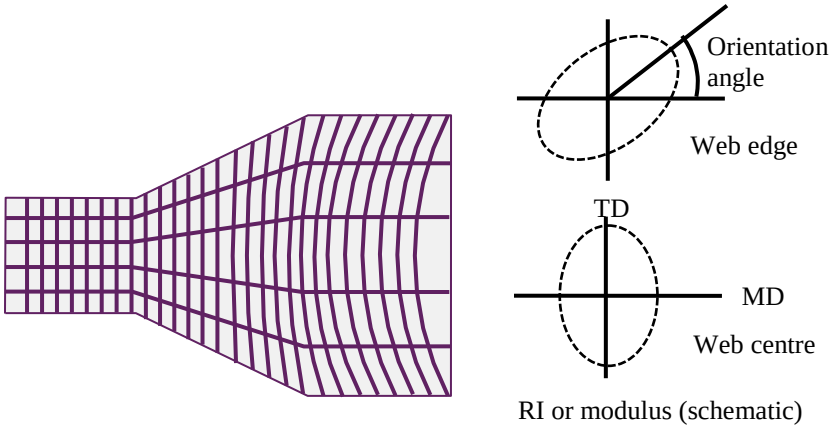

Figure 12 – Schematic diagram of sideways stretching during PET film manufacture, showing distortion of a printed grid. The ellipses at the right sketch the variation of properties such as refractive index and Young's modulus with test direction at the web edge (upper) and center (lower).

At any point, the angular dependence of several properties follows that of the appropriate tensor, with just 3 or 4 parameters needed to describe it [19]. Most properties have their maxima and minima at 90° intervals along the orientation axes. The exception is shrinkage, whose cause is the strain during cooling and any subsequent processing. Its principal axes may shift as the temperature increases, and they do not lie along the orientation axes. Off-axis shrinkage has received very little attention.

Summary

Temperature and moisture both generate a reversible component of dimension change. 0.05% length increase can be caused by either 20 deg C or 70% RH increase.

The viscoelastic response to web handling tensions causes significant dimension change once temperature is increased. Linear viscoelastic theory and TTS allow modelling and qualitative understanding of processes. However, there is shortage of data and validation tests.

Shrinkage is the gradual recovery of strain frozen-in during cooling. Its release is triggered by increased temperature or time-temperature.

Properties are anisotropic with the principal angle changing across the full manufactured width (4 to 9 m). There does not seem to be much pressure to reduce property anisotropy. Partial widths from the center may perform better, but suppliers may be unable or reluctant to be selective about supplying them.

USING SUBSTRATE PROPERTIES TO MODEL PERFORMANCE

The response of a final or intermediate product to deformation, imposed loads and temperatures can be predicted using suitable models and measurements of properties. There are several published studies of the time-dependence of stresses in wound rolls as a result of viscoelasticity, for example [20]. Including the time-response of webs in dynamic models for control has been carried out [21], although these do not appear to follow the history of deformation in the material as it moves through the process. The effect of thermal expansion on stress in a web wrapping a roller, potentially leading to wrinkling or slip, has been modelled [22]. In this paper, the effect of time, temperature and restraint on the bending of a stack of material containing one or more polyester layers is estimated as an example.

Stack Bowing Model

In the manufacture of flexible displays, the active structure is built up by deposition steps onto a polyester substrate. To reduce the effect of dimensional stability on heating, the substrate is fixed to a glass plate, making a panel which is processed using standard electronics industry tools. Some of the steps involve drying and curing, or “baking”, at elevated temperature.

Although held flat during the heating and cooling, on release the panel deforms into a bowed shape, which causes problems for the next stages. It is difficult to mount, and a vacuum table may be unable to pull it down flat. As a result, the deposition geometry is disturbed and the heat transfer through the glass plate to the table becomes non-uniform. The bow becomes unacceptable when the corners or center of a 350 mm square panel lift more than 1 mm. This can occur with baking temperatures as low as 60 deg C.

Similar bowing behavior is observed when the panel consists of polyester, adhesive and glass only: the behavior of the extra deposited layers has only a minor effect. Time and temperature of bake affect bow significantly. Post-bake relaxation and curved formers during bake have been explored. A mathematical model was requested to try and help understand the observations, and to clarify how the bow could be reduced to manageable levels.

The bow is caused by the mismatch of thermal expansion coefficients between the layers and possible irreversible shrinkage of polymer layers above their glass transition temperature. On heating, curvature or thermal stresses develop, but partially decay because of viscoelastic relaxation. On cooling, thermal contraction stresses are generated but do not decay significantly at room temperature. When the panel is free from restraint, it bows to reach a state of ease. Although there are still stresses in the layers, the overall bending moment is zero. The model uses thermal expansion and shrinkage as functions of temperature, together with time- and temperature-dependent viscoelastic properties as described in the first part of this paper.

Model Equations

All layers are assumed to be either isotropic or orthotropic with their principal axes aligned with the panel edges and the MD and TD directions of the film layers. Through-thickness stresses are taken as zero, and thickness changes are ignored. Stress and strain

are taken as uniform over the area of the panel (until the effects of gravity are considered later).

At any time and position, the *x*-component of strain at height *z* from the lower surface is given by:

$$\varepsilon_x = {\varepsilon_x}^0 - k_x z + {\varepsilon_x}^i \quad \{12\}$$

ε_x measures the change relative to the unstressed dimension at 20 deg C. ${\varepsilon_x}^i$ is the initial strain in layer *i* when the stack is formed: for example, it may be laid down under tension. ${\varepsilon_x}^0$ and k_x are shape parameters with a single value through the whole stack. k_x is the *x*-component of curvature, and ${\varepsilon_x}^0$ is a parameter that changes to maintain zero net in-plane force when the panel is free, i.e.

$$\int_0^Z \sigma_x dz = 0 \quad \{13\}$$

The integral is through all layers in the total thickness *Z*. If the panel is free to bend in *x*, then there is zero bending moment and k_x changes to satisfy:

$$\int_0^Z \sigma_x z dz = 0 \quad \{14\}$$

In each layer, the total strain is the sum of thermal, shrinkage, and mechanical components:

$$\varepsilon_x = {\varepsilon_x}^t + {\varepsilon_x}^s + {\varepsilon_x}^m \quad \{15\}$$

Thermal strain ${\varepsilon_x}^t$ is calculated from the temperature history $T(t)$ and the coefficient of linear thermal expansion:

$${\varepsilon_x}^t = \int_{20}^T \alpha_x(T) dT \quad \{16\}$$

The shrinkage strain ${\varepsilon_x}^s$ is taken to be positive if there is expansion, and is obtained from the TMA shrinkage curve. A fitted function or interpolation between tabulated values could be used, but for this work a fit to the same relaxation times as above was used:

$${\varepsilon_x}^s = \sum_{k=1}^{N_k} S_x^k \left(1 - e^{-t_r/\tau_k}\right) \quad \{17\}$$

The reduced time t_r in each viscoelastic layer is obtained from the temperature history and an extension of equation 2:

$$t_r = \int_0^t a(T(t'))dt' \quad \{18\}$$

The mechanical strain ${\varepsilon_x}^m$ is the part of the deformation due to stress.

Equations 12 to 17 have counterparts for the *y*-components.

The viscoelastic constitutive equations are discretized using techniques similar to those described in references [20] and [23]. The current time t_j is subdivided into *j* intervals. Each integral in equations 6 and 7 takes the form:

$$I = \Delta\varepsilon^m{}_j \left\{ C_0 + \sum_k \frac{C_k \tau_k}{\Delta t_{rj}} \left(1 - e^{-\Delta t_{rj}/\tau_k}\right) \right\} + C_0 \varepsilon^m{}_{j-1} + \sum_k C_k \, \tau_k \beta_{kj} e^{-\Delta t_{rj}/\tau_k} \quad \{19\}$$

x and *y* suffices have been dropped for clarity. The reduced time is calculated using analytic integration of equation 18 for the sequence of constant temperature and linear ramp processes. The memory terms are updated after each timestep:

$$\beta_{kj+1} = \beta_{kj} e^{-\Delta t_{rj}/\tau_k} + \frac{\Delta\varepsilon^m{}_j}{\Delta t_{rj}} \left(1 - e^{-\Delta t_{rj}/\tau_k}\right) \quad \{20\}$$

Several sets of memory terms are needed: each viscoelastic layer in the stack requires 8 to follow all the mechanical strain terms in equations 6 and 7, four for the constants and four for the gradients through the thickness k_x ,k_y.

Changes in restraint are assumed to happen instantaneously, with equations 19 and 20 adapted for a zero timestep.

The change in mechanical strain is derived from equation 12 to 15. If the panel is fixed, there is no change in the shape parameters $\varepsilon_x{}^0$, $\varepsilon_y{}^0$, k_x or k_y, so the integrals can be evaluated to calculate the stress components. When the panel is free to expand when flat, or bow in one or both directions, at least 2 of the shape parameters are unknown. Applying equations 13 and 14 as needed results in simultaneous equations whose solution gives the changes in the shape parameters.

Implementation

In the Excel® model, the user inputs the name and thickness of each layer in the stack (up to 12). The name refers to a material property data range, giving the elastic, viscoelastic, thermal expansion and shrinkage parameters for that material. The duration, start and end temperature of each part of the sequence are entered in a table, and the restraint conditions selected.

20 equal timesteps were used in each part of the sequence of temperature changes. For cooling, this was increased to 100 for improved accuracy. For the final period, when bow is developed, successive steps were increased by a factor of 1.3 to enable the initial bow to be displayed, and compared with the bow hours later.

If the panel has a tendency to bow in both *x* and *y* directions, it may show curvature in either one or both directions. Most commonly, the higher curvature develops and the panel remains straight in the other direction. A definite criterion has not been established, but double curvature is favored if the parameter $l/\sqrt{RZ} < 1$. l is the maximum panel dimension, *R* the smaller of the bow radii, and *Z* the total thickness. Only if the panel is small enough, both curvatures develop. Example graphical output in figure 13 shows the decay in *x* and *y* curvatures with time, for singly- and doubly- curved behavior.

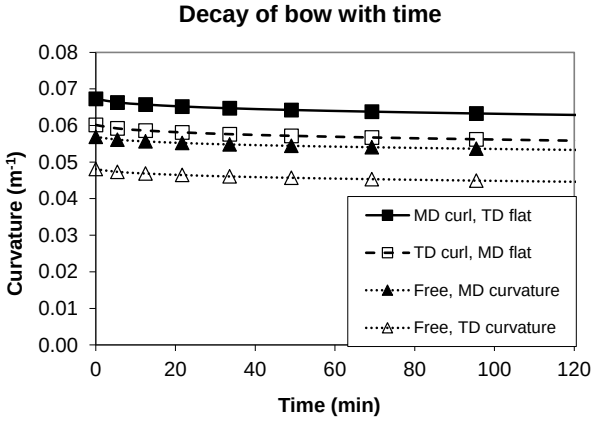

Figure 13 – Example output of the model: MD and TD curvature change with time after release following a thermal cycle. Top 2 curves show single curvature in MD then TD; bottom 2 curves show MD and TD curvatures for doubly-curved.

Each single curvature is converted to end height, and the reduction due to gravity calculated assuming the center of the panel rests on a surface [24], as demonstrated in figures 14 and 15.

Figure 14 – Sketch of reduction in height due to increasing gravity effect.

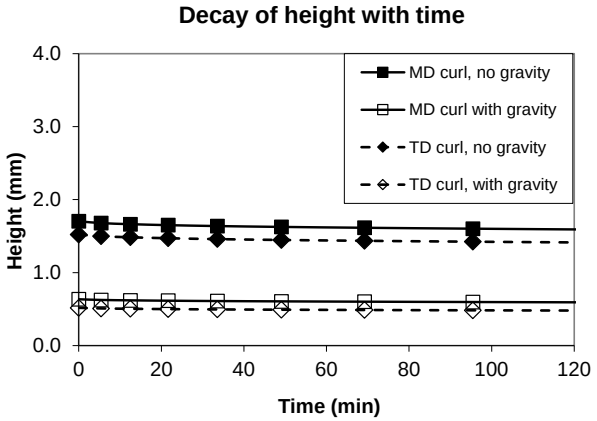

Figure 15 – Example output of the model: the effect of gravity on the edge height of a panel resting on a flat surface in MD and TD. Solid markers – curvature alone; hollow markers – with gravity acting.

Model Application

The bowing problem was explored experimentally using narrow test panels with simplified structure at Plastic Logic's laboratories. The stack structure is shown in table 1, and the properties of the elastic layers in table 2.

Layer no.	Material	Thickness (μm)
1	Glass	1100
2	Adhesive	48
3	PET film	100
4	Adhesive	48
5	PET film	100

Table 1 – Layers in the stack bow model.

The adhesive layers have low stiffness and act as spacers, but are able to transmit stresses, so that the panel bends without shear. Shrinkage strains were set to zero because temperatures never reached the range where shrinkage is active. The layers were added under zero tension, so initial strains were also set to zero.

	Glass	Adhesive
Young's modulus (GPa)	62.8	0.01
Poisson's ratio	0.2	0.4
Coefficient of linear thermal expansion (K^{-1})	3.5×10^{-6}	10^{-4}

Table 2 – Elastic layer properties.

The test strips were oriented in the PET film TD direction, 350 by 60 mm in size and held with 20 mm of the long dimension clamped during examination of the bow with the short dimension vertical to eliminate deflection due to gravity. Baking was conducted for 1 hour in an oven at the prescribed temperature. The placement and removal of the strip clamped to a flat or curved plate was simulated by a steady temperature ramp over 1 minute. The model results were insensitive to changes of ramp rate.

Effect of baking conditions

Figure 16 shows the experimental and model results for bow after heating, holding for 1 hour under restraint on a curved or flat rigid former, then cooling and measuring bow.

For 60 deg C bake there is good agreement between the experimental results and model prediction. When baked flat, the bow is 1.5 mm, but this can be reduced to almost zero by holding on a former with radius 915 mm.

Baking flat at 70 deg C gives an increased bow of 3.2 mm. Using the curved former again reduces the bow. The model overpredicts the amount of bow by around 2 mm for all formers but the dependence on radius is correct, apart from this offset.

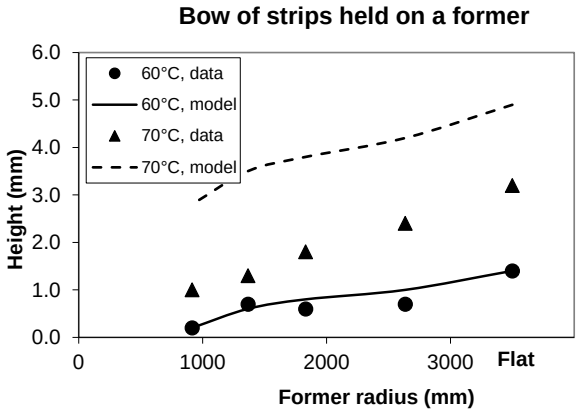

Figure 16 – Measured and predicted bow of strips after thermal cycling to 60 and 70 deg C while held on a curved former or flat.

Using post-bake relaxation

In a second set of experiments, the initial bake was for 1 hour at 70 deg C. The test strips remained clamped flat while they were relaxed at an intermediate temperature of 20 to 50 deg C for 57 hours. The results are shown in figure 17. The bow is reduced by the extra relaxation step. The experiments show that the strongest reduction in bow is made by relaxing at 20 deg C.

The model slightly under-predicts the amount of bow before relaxation. It also predicts an improvement with relaxation, but the effect of temperature is opposite to the experiments. Higher temperature is predicted to have a greater effect, which is perhaps more in line with expectation, but does not fit the data. The change in bow at 20 deg C is predicted reasonably well for the initial 57 hours and after a further 7 days.

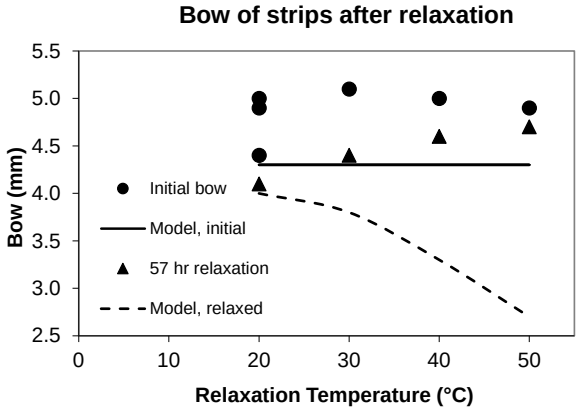

Figure 17 – Measured and predicted bow of strips before and after relaxation for 57 hr at the temperatures shown.

Conclusions

The model predicts the correct direction of bowing, and experimental trends, but its absolute accuracy is not perfect, possibly because of moisture expansion and relaxation effects. The measurement reproducibility is not perfect (figure 17). Other possible reasons are shear and/or slip in the adhesive, and the neglect of a planarizing acrylic coating layer on the film surface.

The model is helpful for:

- Predicting the bow of different panel sizes.
- Avoiding severe conditions of bake time and temperature.
- Forecasting the effect of material changes such as thickness, modulus, expansion and shrinkage.
- Reducing bow with a relaxation step or holding in a curved shape.
- Predicting bow after one layer is removed, or the stack is removed from the glass.
- Estimating dimension changes during and after bake.
- Assessing bow at higher temperature. Residual film shrinkage becomes significant for baking above 80 deg C. Heat-stabilized film offers some benefit but will not eliminate bow.
- Assessing the benefit of moving to the more expensive poly(ethylene naphthalate) substrate.

It is clear that mounting the device on a stiff carrier does not remove dimensional stability problems, but does reduce them and makes the panel easier to lift and place.

Models of this type can be used to investigate many issues where dimensional stability is an issue. One example is the setting in of curl when a flexible device is rolled up for a long time [24]. Upon release, it does not flatten completely but the curl recovers gradually.

A further example is curl and dimension change induced by roll to roll processing. Temperature, MD strain and bending radius vary with time as a web element moves along the line. However, in this case it is likely that through-thickness variations of temperature need to be considered to follow the thermal diffusion through the thickness when contact is made with a roller.

DIMENSION CHANGES DURING WEB PROCESSING

When the web moves through a line and experiences changes in tension and temperature, its dimensions change as a result of viscoelastic deformation, thermal expansion and contraction, and the development of shrinkage. To a first approximation, these are additive.

Difficulties frequently arise when the web passes through an oven, with a long free span during which the temperature rises and falls. This can introduce a change in the web dimensions causing registration errors, and wrinkles that are set in.

It is useful to sketch out the width changes assuming zero TD stress, and then consider whether the web edges will follow that path or not. An imaginary tape element at the web edge prefers to travel straight to minimize its stretch relative to the web center. However, the edges will move inwards to follow a width contraction, as the free web cannot sustain significant TD tension. By contrast, a web expansion can be accommodated by forming troughs in the MD with the edges travelling straight.

The web will achieve close to its predicted width on the roller at the oven exit. Friction can allow a small TD stress to develop [25], but the effect on width is small

compared with other changes. Troughs coming onto the roller will normally spread out; but if the web is thin and there is good traction, narrow wrinkles may pass over the roller.

Broadly speaking, a convex width prediction will be followed; but the edges will straighten out a concave path, and troughs will form. If these troughs are present when the web cools, their shape will be "frozen-in". Troughs are less likely in an air flotation oven, where the sinusoidal web path provides shape-stiffening and a true width increase may occur.

Examples

The deformation mechanisms normally act together, but it is instructive to separate them in order to understand their effects. In all cases, there is a long web span where the web heats and cools without touching any rollers before the exit back at ambient temperature. The sketches show the width variation before the edges have been "straightened out".

Thermal expansion at low tension (Figure 18). The MD mechanical strain is low at all times. Thermal strain during heating causes expansion in both MD and TD, but that is recovered during cooling. There is no change in the unstressed dimensions. However, the web width increase when hot tends to generate troughs.

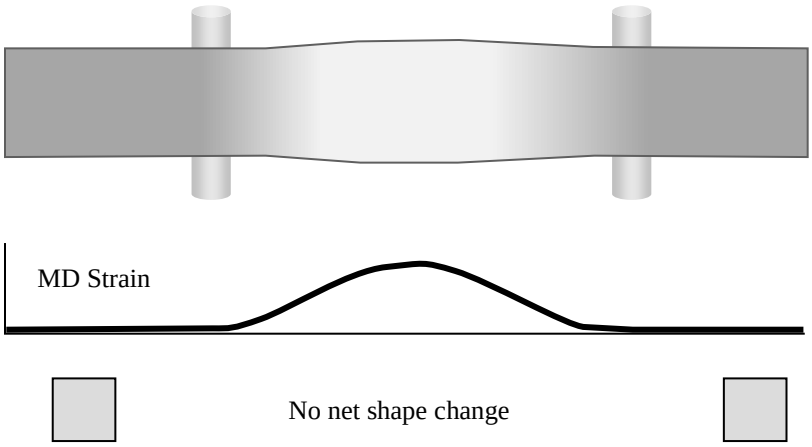

Figure 18 – Web width and MD strain changes from thermal expansion alone, during heating and cooling in an oven.

High tension (Figure 19). The MD mechanical strain increases considerably because of viscoelastic creep at high temperature. The stress is still present during cooling so there is no recovery. Later, removing the tension causes a fall in MD strain, but only the same amount as the tension caused originally when cold. There is therefore an increase in MD length from the high tension and temperature. The width falls in proportion to the extra strain from creep, smaller by a factor of Poisson's ratio. This TD contraction is not recovered so a TD contraction accompanies the MD expansion.

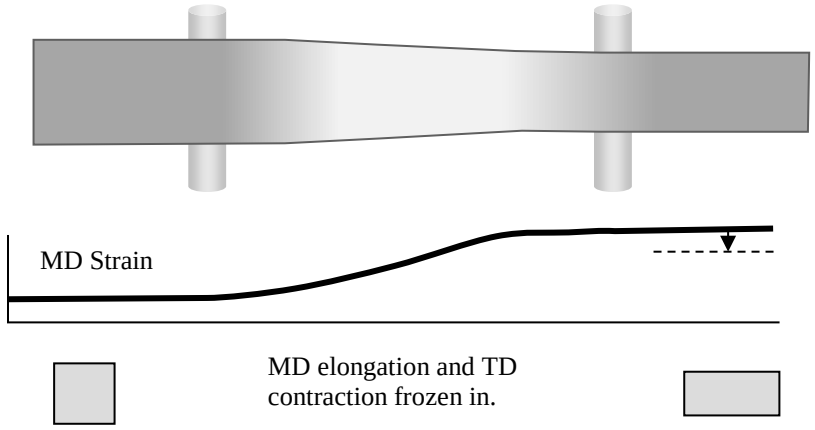

Figure 19 – Width and MD strain changes from high tension during heating and cooling in an oven.

Low tension (Figure 20). If the tension is reduced from a high level by driving the oven entry roller, the web width will expand as it leaves the roller. This may cause troughs early in the oven. However there is no effect on the unstrained web dimensions, as long as the tension is low enough.

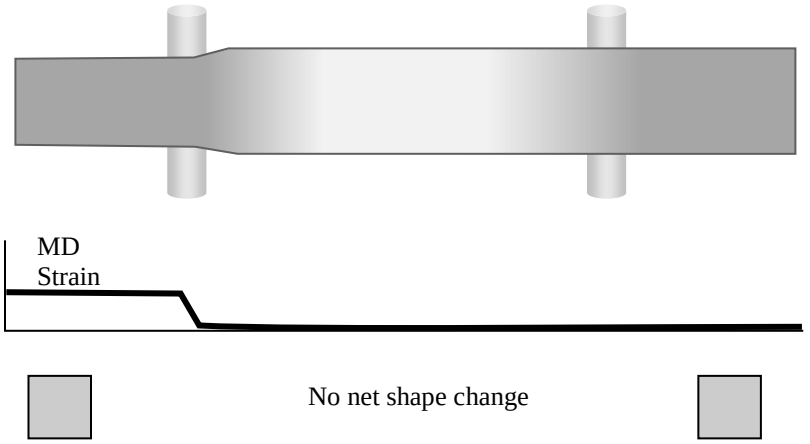

Figure 20 – Width and MD strain changes from a reduction in tension over the entry roller followed by heating and cooling in an oven, with likely occurrence of troughs or wrinkles.

Shrinkage in both MD and TD (Figure 21). When the web becomes hot, it contracts in both MD and TD. The web dimensions are reduced. The web width starts to fall some distance into the oven, and this pulls the web edges inwards up to that point. As a result, troughs may be generated in the heating region.

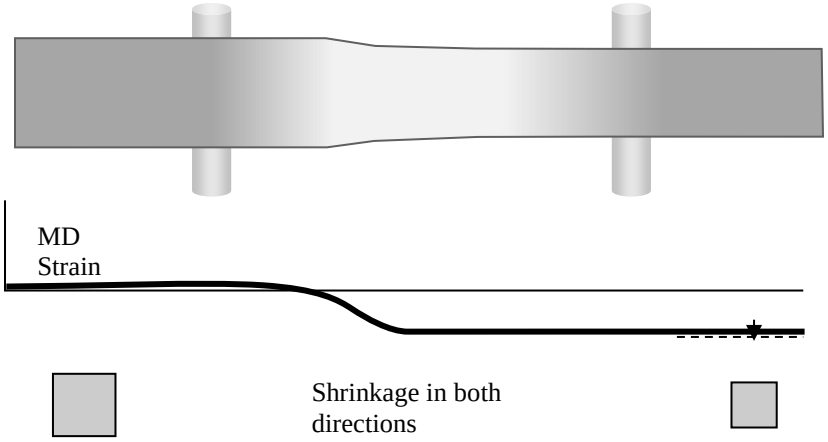

Figure 21 – Web width and MD strain changes from shrinkage in both directions, during heating and cooling in an oven.

MD shrinkage and negative TD shrinkage (Figure 22). The web may have these properties as a result of heating and cooling under high tension (Figure 19). After passing through the oven, the web is shorter in the MD but wider in the TD. In the oven, the tendency to increase width stops once the maximum temperature is reached. The edges tend to move in a straight line from the narrower inlet width to the final exit width, and so there is a tendency to form troughs once expansion starts.

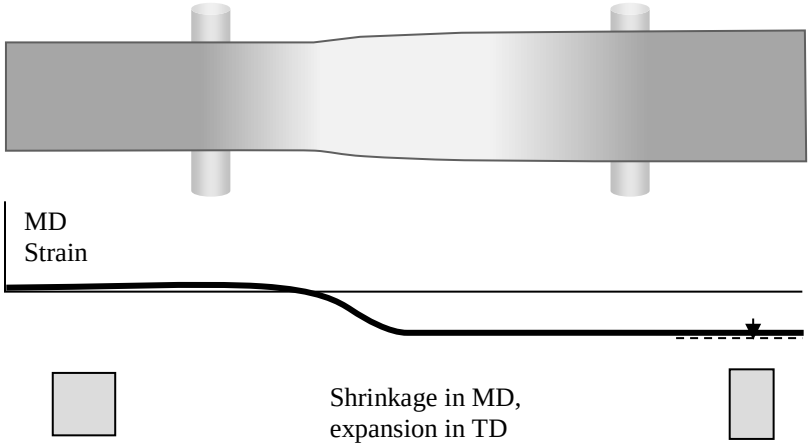

Figure 22 – Web width and MD strain changes from positive MD and negative TD shrinkage, during heating and cooling in an oven.

Discussion

This method can be made more quantitative by estimating the magnitudes of dimension changes using the viscoelastic, thermal expansion and shrinkage data. Shrinkage should be measured on the particular material being used: it may develop

gradually as temperature increases, or remain small up to the temperature where the material was earlier heat-stabilized and develop strongly thereafter.

It is important to know the web temperature through the oven. Convective air heating, radiant infrared elements or heated platens are used. The web temperature can be measured with a pyrometer, or predicted using heat transfer theory (with drying if there is a wet coating on the surface). Considering the width variation can help guide the selection of set temperatures, particularly in intermediate cooling zones.

Troughing in the oven is common. Making the exit roller a spreader could give a benefit by increasing the width in the last part of the free span. However, it will have limited benefit if the wrinkles originate near the entry. Spreading devices such as edge nips and D-bars could be placed in the oven: consideration of the width changes enables them to be placed at the optimum location.

Conclusions

- MD tension causes creep at elevated temperatures, accompanied by TD width reduction.
- Both these dimension changes are frozen-in on cooling
- Thermal expansion gives reversible dimension change, but that from shrinkage is irreversible.
- The web edge can follow a straight or concave path to follow width variations.
- The edge runs straight rather than follow a convex width, but the web forms troughs rather than moving into TD compression.
- Troughs may cause problems: they are set in by cooling, and troughs in thin webs may run over the exit roller as wrinkles.

ACKNOWLEDGEMENTS

The DMA and TMA measurements were carried out by Andrew Broadhurst of Intertek MSG, Wilton Centre, UK. DuPont Teijin Films and Plastic Logic staff helped steer the bow model development, provided data, and gave permission to present.

REFERENCES

1. Nathan, A., et al., “Flexible Electronics: The Next Ubiquitous Platform,” Proc. IEEE, Vol. 100, May 13, 2012, pp. 1486-1517.
2. Crawford, G.(ed.), Flexible Flat Panel Displays, John Wiley and Sons, 2005.
3. Organic and Printed Electronics Roadmap, 6th Edition, Organic and Printed Electronics Association, Frankfurt-am-Main, Germany, 2015, www.oe-a.org.
4. MacDonald, W. A., Looney, M. K., MacKerron, D., Eveson, R., Adam, R., Hashimoto, K., and Rakos, K. “Latest Advances in Substrates for Flexible Electronics,” J. Soc. for Information Display, Vol. 15, No. 12, 2007, pp. 1075-1083.
5. Bhushan, B., Mechanics and Reliability of Flexible Magnetic Media, Springer-Verlag, 2nd ed., 2000.
6. Tsunashima, K., Toyoda, K., and Yoshii, T., “Stretching Conditions, Orientation and the Physical Properties of Biaxially Oriented Films,” Film Processing, ed. Kanai, T. and Campbell, G.A., Hanser Publications, Cincinnati and Munich, 1st ed., 1999, pp. 320-352.
7. Ferry, J. D., Viscoelastic Properties of Polymers, John Wiley and Sons, 3rd ed. 1980.

8. ASTM D882 – 12, “Standard Test Method for Tensile Properties of Thin Plastic Sheeting,” 2015.
9. TA Instruments DMA Q800.
10. Bogy, D. B., Bugdayci, N., and Talke, F. E., “Experimental Determination of Creep Functions for Thin Orthotropic Films,” IBM J. Res. Develop., Vol. 23, 1979, pp. 66-74.
11. Williams, M. L., Landel, R. F., and Ferry, J. D., “The Temperature Dependence of Relaxation Mechanisms in Amorphous Polymers and Other Glass-Forming Liquids,” J. Amer. Chem. Soc., Vol. 77, 1955, pp 3701-3707.
12. Greener, J., Tsou, A. H., Ng, K. C., and Chen, W. A., “The Bending Recovery of Polymer Films I: A Phenomenological Model,” J. Poly. Sci. Part B: Polymer Physics, Vol. 29, 1991, pp 843-858.
13. Perkin Elmer Model 7 Thermomechanical Analyzer.
14. Unpublished work.
15. Yasuda, H., and Stannet, V., “Permeation, Solution and Diffusion of Water in Some High Polymers,” J. Poly. Sci., Vol. 57, 1962, pp. 907-923.
16. Blumentritt, B. F., “Anisotropy and Dimensional Stability of Biaxially Oriented Poly(Ethylene Terephthalate) Films,” J. Appl. Poly. Sci., Vol. 23, 1979, pp. 3205-3217.
17. Bhushan, B., and Connolly, D., “Viscoelastic Properties of Poly(Ethylene Terephthalate),” ASLE Trans., Vol. 29, 1986, pp. 489-499.
18. Jones, D. P., MacKerron, D. H., and Norval, S. V., “The Anisotropy of Thermal Expansion in Polyethylene Naphthalate,” Plastics, Rubbers and Composites: Materials and Applications, Vol. 42, No. 3, 2013, pp. 66-74.
19. Chan, A., and Smith, T. L., “Anisotropy of the Coefficients of Linear Thermal Expansion and Other Properties of Six Biaxially Oriented Films of Poly(Ethylene Terephthalate),” IBM Research Report, no. RJ 269 (34184), October 1979.
20. Qualls, W. R., and Good, J. K., “An Orthotropic Viscoelastic Winding Model Including a Nonlinear Radial Stiffness,” Trans. ASME J. Appl. Mech., Vol. 64, 1997, pp. 201-208.
21. Carlson, D. H., Pagilla, P. R., and Weaver, M. D., “Modelling and Control of Web Velocity and Tension: An Industry/University Perspective on Issues of Importance,” Proceedings of the Tenth International Conference on Web Handling. Ed. Good, J. K., Oklahoma State University, 2009, pp. 197-217.
22. Jones, D. P., McCann, M. J., and Abbott, S. J., “Web Tension Variations Caused by Temperature Changes and Slip on Rollers,” Proceedings of the Eleventh International Conference on Web Handling, Ed. Good, J. K., Oklahoma State University, 2011, pp. 65-84.
23. Reference 5, pp. 321-2.
24. Jones, D. P., “Curl Measurement, Causes and Models,” Presented at AIMCAL Technical Program at the International Converting Exhibition Europe, Munich, Germany, March 2013 (unpublished).
25. Shelton, J. J., “Buckling of Webs from Lateral Compressive Forces,” Proceedings of the Second International Conference on Web Handling, Ed. Good, J. K., Oklahoma State University, 1993, pp. 304-321.